Characterization of Coplanar Waveguide Ringresonators for Circuit QED Applications

Raphael Barmettler

February/March 2011

Three weeks laboratory work in the Group of Andreas Wallraff at the
Quantum Device Lab, ETH Zurich
Supervisor: Lars Steffen

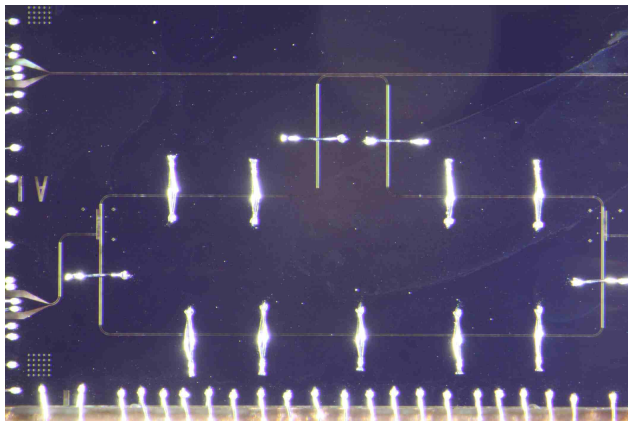

Abstract

In this report the microwave transmission spectrum of a coplanar waveguide capacitively coupled to a ring resonator is characterized. Therefore the transmission is measured for different sample geometries and different bond configurations and the results of the different measurements are compared to each other. The measurements are also compared to computer simulations of the microwave spectrum. This results are interesting for circuit QED applications, because in contrast to the widely used linear resonators, a standing wave in a ring resonator has no defined phase.

Contents

1 Introduction

In the last years quantum computing has become a very important topic in science. The goal is to produce a computer, which is not based like a classical computer on classical physics (transistors), but on quantum mechanics. Instead of a classical bit, which can just assume the values 1 or 0, a qubit can assume a superposition of both states. This qubit must be a quantum mechanical two level system. There are different candidates for such a qubit, for example superconducting circuits, trapped ions, quantum dots etc.

One type of superconducting circuits qubits, called charge qubit, consists of a superconducting island, with or without a cooper pair on it. More information about charge qubit can be find in [1]. The qubits can couple capacitively to their environment. Therefore, if placed in a microwave resonator, they can couple to the electromagnetic field modes of that resonator. This so called circuit quantum electrodynamics (cQED) setup can be used to control and read out the qubit state [2][3] or to couple many qubits to each other [4]. The resonators used so far in cQED experiments are linear half-wavelength resonators, but in this experiment a new kind of resonators, ring resonators, are tried to characterize. The advantage of a ring resonator over a linear resonator is, that the qubits can be positioned everywhere in the ring and couple to the electric field (section 2.2). The goal of this experiment is to understand the microwave properties of a ring resonator without qubits for different geometry set-ups and different numbers of bond wires. Therefore the transmission is measured and compared to a computer simulation.

2 Theory

2.1 Coplanar Waveguide

A waveguide is an structure, which conveys electromagnetic waves between its endpoints. To analyze the electric and magnetic field in the waveguide Maxwell's equations are used with boundary conditions defined by the materials of the waveguide [5]. An important quantity is the impedance. It is defined as

$$Z = \frac{E}{H}, \tag{1}$$

where E is the electric and H the magnetic field. In vacuum the impedance Z is equal to 377 Ω [6]. In a waveguide it depends also on the geometry and the magnetic and dielectric constant of the materials. A common standard for a waveguide is an impedance of 50 Ω.

Figure 1: Schematic representation of a coplanar waveguide. The green area represent a dielectric material, the blue area a metal and the white area is air.

A coplanar waveguide consists of a dielectric ground and a metallic plane on the top. At two parallel running lines the metal is etched like described in chapter 3.2. Therefore there is a center metallic conductor, which is not connected to the metallic plane. Fig. 1 shows a schematic representation of such a coplanar waveguide. The electric and magnetic field are in the situation of a ideal metal only in the dielectric material and in the air between the center conductor and the top plane.

2.2 Resonator

In this experiment there are two coplanar waveguide involved. First a so called feed line. It is connected to a network analyzer, which sends microwave through the feed line and measures the transmitted waves on the other endpoint.

Near to this feed line is the ring resonator. It consists also of a coplanar waveguide, but it is a closed loop with no direct connections to a network analyzer. But if the frequency in the feed line matches a resonance frequency in the loop, the microwaves are absorbed by the ring.
The resonance frequency of the ring depends on the dielectric constant of the material and the length of the ring. It holds

$$\nu_0 = \frac{c}{\sqrt{\epsilon_{\text{eff}}} \cdot l}, \tag{2}$$

where l is the length of the ring resonator, c is the speed of light in the vaccum and ϵ_{eff} is the dielectric constant [7]. The wavelength at resonance is in contrast to a linear resonator equal to the length of the ring ($\lambda_0 = l$). A linear resonator is a straight running waveguide capacitively coupled to two feed lines at its endpoints. Microwaves only transmits, if the resonator is in resonance. The resonance wave length in such a linear resonator is twice the length of the resonator ($\lambda_0 = 2 \cdot l$). The wave in a resonator is stored as a standing wave. The advantage of the ring resonator over the linear resonator is, that it has no endpoints and therefore there is no boundary conditions for the E-field. The maximum of the standing wave is not in a fix position on the ring, but can move and the phase of the wave is not determined by the geometry. This is an important property for quantum computation, because the qubit can be positioned at any point in the ring and can nevertheless couple to the electromagnetic field.

The ring resonator will absorb microwaves as a function of its frequency. Near to a resonance frequency there is more absorption than in a non resonance frequency. The following ansatz of a driven harmonic oscillator is used for the transmission through the feed line:

$$y_0 + A_0 \frac{\delta\nu^2}{\delta\nu^2 + (\nu - \nu_0)^2}, \tag{3}$$

where y_0 is the transmission in the case of no resonance, ν is the frequency in the feed line, ν_0 is the resonance frequency of the ring, $\delta\nu$ is HWHM (Half Width at Half Maximum) and A_0 is a constant. Such a function is called a Lorentzian function. In the case of the ring resonator A_0 is always negative, because it absorb the wave at its resonant frequency. The quality factor (Q factor) is defined as

$$Q = \frac{\nu_0}{\delta\nu}. \tag{4}$$

It is expected to decrease as a function of the frequency.

3 Experimental Set-Up and Measuring Technique

3.1 Samples Set-Up

3.1.1 General Set-Up of the Samples

The dielectric material in this experiment is sapphire (crystalline Al_2O_3). The metallic top plane is made of niobium (Nb). It is the 41^{th} element in

the periodic table and it is a transition metal. Niobium becomes a superconductor at a temperature of 9.2 K (at atmospheric pressure) and is therefore the element with the highest critical point of superconductivity [8]. Since the experiments will be performed in a bath of liquid He (T=4.2 K), all Nb structures will be superconducting.

The central conductor of the coplanar waveguide is not connected to the two metal planes on its side. The two metal planes are grounded, but they are not directly connected to each other, what changes the electric potential of the plane and therefore also the resonant frequency of the ring. To solve this problem of the potential different, bond wires are added at different positions on the wave guide. Bond wires are small wires on the metallic plane, which connect the planes on both side of the wave guide, but not the central conductor. The bond wires used in this experiment are made of aluminum (Al). Aluminum turns to a superconductor at 1,2 K and its resistivity at 4 K is 0.82 $\cdot 10^{-3}$ $\mu\Omega$m [9].

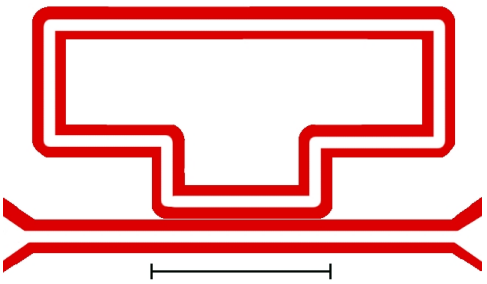

Figure 2: Schematic Representation of the samples geometry. The red lines symbolize sapphire and the white plane niobium. The length are not true of scale.

The ring resonator used in this experiment is not round, but has the shape like schematically showed in Fig. 2. The red parts symbolize the dielectric material (sapphire) and the white plane the metal (niobium). The center conductor has a width of 10 μm and the width from the center conductor to the metal plane is 4.5 μm. The distance, where the ring resonator and the feed line are running side by side, is 500 μm. The length of the whole ring resonator is 14.820 mm, what leads with Eq. 2 to a calculated resonant frequency of 8.2 GHz.

Sample name	Gap/Wall	Distance	2/4-Ports,Q
I1	Gap	4 μm	2-Ports
A1	Gap	4 μm	4-Ports, Q
K1	Gap	9 μm	2-Ports
J1	Gap	6 μm	2-Ports
N1	Wall	5 μm	2-Ports
G1	Wall	4 μm	4-Ports, Q

Table 1: Properties of the samples

3.1.2 Specific Set-Up of the Samples

There are six different samples used in this experiment. They are called Mask13A1, Mask13N1, Mask13J1, Mask13K1, Mask13G1 and Mask13I1 in short A1, N1, J1, K1, G1 and I1. Every of them has the properties like described in the subsection 3.1.1, But each of them is different from the others. Tab. 1 shows the properties of each sample. Gap and Wall stand for the kind of contact between the resonator and the feed line. In samples labeled as Wall there is a ground plane between the coplanar waveguide of the resonator and the coplanar waveguide of the feed line like showed in Fig. 3 b). In the samples labeled with Gap, there is no ground plane between the center conductor of the feedline and the center conductor of the resonator. Like showed in Fig. 3 a).

The third column of Tab. 1 shows the distance between the resonator and the feed line. This is the thickness of the metal in the case of a wall-type sample or the distance between the center conductors for the Gap-type samples.
Qubits in a resonator are in a gap in the ground plane near to the resonator, which are connected to the network analyzer. None of sample used in this experiment has a qubits in its resonator. But A1 and G1 are labeled in Tab. 1 with "4-Ports,Q", what means, they have two empty qubit gaps. They are positioned on the right and left side of the resonator. Therefore A1 and G1 has four ports: two at the feed line and one at any empty qubit gaps.

The number of bonds is always increased between two measurements. Pictures of every sample and the positions of the bonds at the different measurements sequenze are showed in the appendix.

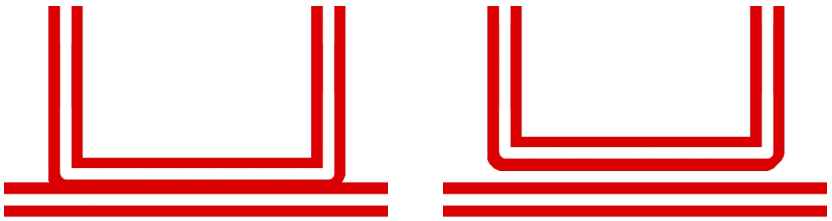

Figure 3: Zoom of Fig. 2 to the connection of the resonator to the feed line of a sample with a) a Gap and b) a Wall

3.2 Photolithography

The samples used in this experiment are made by the technique of photolithography. First the metal (niobium) is sputtered to the dielectric (sapphire). Than the metal is covered with a material called photoresist, which is not stable against UV-light. Than the sample is expose to UV-light at the position, where the metal should be etched off. At this position the photoresist change its chemical properties and is soluble by a solvent. This kind of photolithography, where the exposed parts are etched, is called positive photolithography. The sample is now etched by chemically reactive plasma. The parts under the photoresist are protect and just the exposed metal is evaporated. The advantage of chemically reactive plasma over a liquid acid is, that the plasma etches anisotropically. And so just the metal lying directly under a photoresist free position is evaporated. At the end the photoresist is not needed anymore and is also solubilized by a liquid. Fig. 4 shows a schematic representation of the whole operating sequence. For a closer look, see [10].

3.3 Measuring Technique

All the effects of resonants can just be seen at low temperatures. Is the temperature to high, the signal is too noisy. Therefore the sample is during the experiment in a dipstick in a helium dewar. The ports of the feed line (and the two additional ports of A1 and G1) are connected to coaxial cables, which run in the dip stick. A coaxial cable is a type of a wave guide, where the inner metallic conductor and the outer metal are coaxial. At the end of the dip stick the cables are connected by other coaxial cables to a network analyzer. The network analyzer sends microwaves thought one port and measures the transmission at all the other ports and the reflexion to the

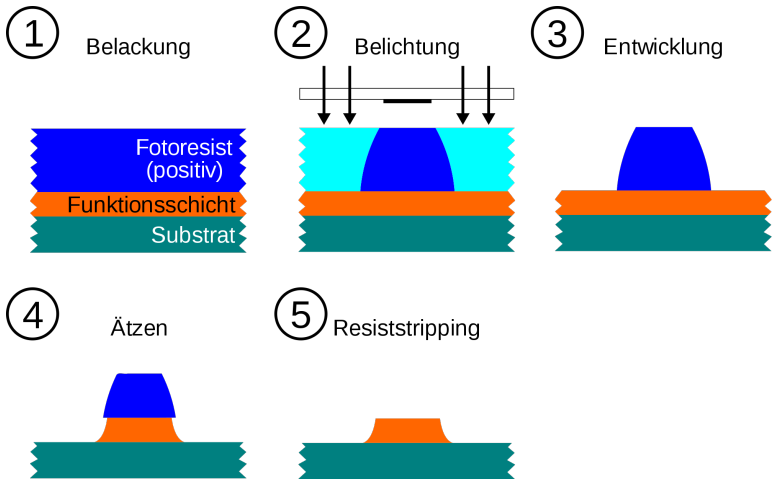

Figure 4: Operating sequence of photolitohography. From [10]

same port. The frequency of the microwave is decreased in 20000 steps from a minimum to maximum frequency. The full spectrum is measured from nearly 0 Hz to 20 GHz. To reach a better resolution at the resonants frequency the minimum and maximum frequency is also adjusted manually around the resonants points. After this 20000 steps the network analyzer do the same with the next port. This sequence is repeated over and over again.

The coaxial cables in and to the dip stick effect also the reflexion and the transmission . Therefore the cable need to be calibrated. The network analyzer has a application to calibrate the cables to the dip stick. Therefore all cables are disconnected from the dip stick and are connected to a calibration box, which connect the cables automatically with different resistance. The network analyzer measures the effect of the cables and will it subtract in all the following measurements.
The cables in the dip stick can not be calibrated by the network analyzer. Therefore the coaxial cables in the dip stick are bypassed at the end and the transmission is measured. This calibration has also to be subtracted from the raw data. The calibration as a function of the frequency is showed in Fig. 5. For high frequency the signal starts oscillating, what could be caused by standing waves in the connecting piece between the two cables in the dipstick. Therefore the data are fitted by a ansatz from [11]. The fitting curve holds

$$C(\nu) = -0.2739 \cdot \nu^{-0.0181} - 3.2831 \cdot \nu^{0.5618} \tag{5}$$

and is represented by the red line in Fig. 5. $C(\nu)$ is already subtracted in all results following in this report.

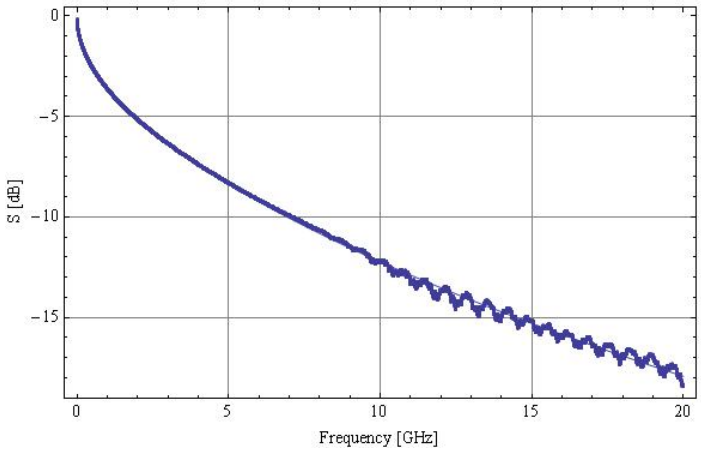

Figure 5: The measured calibration function $C(\nu)$ (blue points) and its fitting curve (red line)

4 Measurement

The first measurements are made on sample I1 with different bond configurations (see appendix). After this measurements the other samples are chosen, such that they differ in just one property, if this is possible (see Tab. 1). So the influence of the different properties of the samples is hoped to be able to analyze. The sample G1 is introduced not until the last measurement. So there is just a measurement with one bond configuration. G1 is chosen to be compared to the samples A1 and N1 (see Tab. 1).

4.1 Without bonds

After choosing the four samples to compare with I1, the next step is to measure the transmission without any bonds on the samples. The full transmission spectrum of this four samples without bonds can be seen in Fig. 6. The transmission is given in the logarithmical unit dB. Hence 0 dB means full transmission.
From Eq. 2, it is expected, that there are two resonance points, one when the wave length is equal to the length of the ring at 8.2 GHz and when the

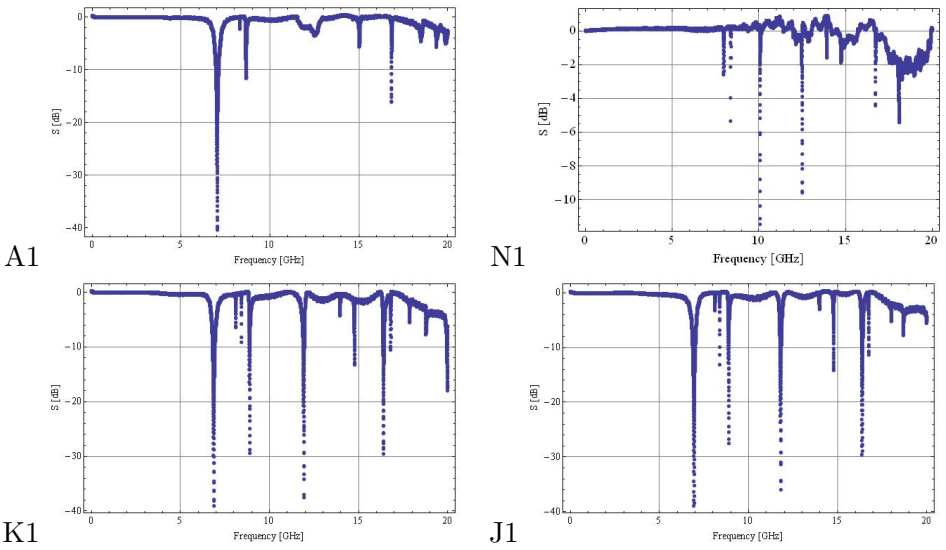

Figure 6: Full transmission spectrum for the samples A1, N1, K1 and J1 without any bonds

	ν_0	$\delta\nu$	Q-factor
A1	7.03107	0.24328	14.4505
K1	6.88018	0.191859	17.9303
J1	6.9252	0.236088	14.6666
N1	7.9683	0.006514	611.629

Table 2: The first peak in the transmission spectrum without bonds

length of the ring is two times the wave length at 16.4 GHz. The transmission should be Lorentzian shaped at the resonance points like described in Eq. 3 and zero dB anywhere else. Tab. 2 shows the position, HWHM and the Q-factor of the first resonance point of the spectrum. The values are determined by fitting with the ansatz from Eq. 3. As a example Fig. 7 shows the data and the fitting curve of the first peaks of the sample N1.

The spectrum of K1 and J1 are very similar, what is the first indication, that the distance between the feed line and the ring resonator has not such a big influence to the resonance spectrum than the other properties of the samples. There are many resonance points in the spectrum, but the first and also the strongest resonance point is around 7 GHz, what could be the

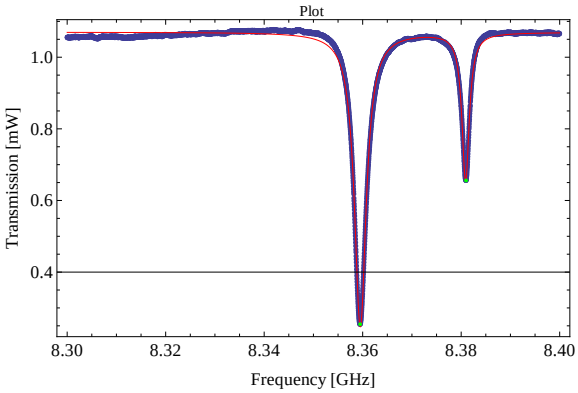

Figure 7: The transmission data (blue) and the fitting curve (red) of sample N1 without any bonds. The green points mark the position of the minima.

first mode of the expected spectrum.
The spectrum of N1 looks different from J1 and K1, what indicates, that the kind of coupling (wall or gap) between the feed line and the resonator is important. But like in K1 and J1 there are many resonance points, but the first is also not until 7.9 GHz. The resonants are weaker than in the other sample with a gap between the resonator and the feed line.
The spectrum of A1 has clearly less resonance points. There is a three-way peak around 8 GHz and a two-way peak around 16 GHz, like expected for the spectrum. This indicates, that the qubit ports might suppress unwanted resonances.

4.2 Bonds over the Ring

In the next step bonds were added around the ring, except for the region with contact to the feed line. Pictures of the samples are showed in the appendix Fig. 13. The transmission of sample A1 is now measured at all four ports of the sample. This means, that also the gate lines for the qubits are connected to the network analyzer. The first measurement of I1 is also compared to this measurement sequence, because it has a similar bond configuration on it. There are fewer bonds on the ring, but one bond at the contact between the feed line and the resonator.

The transmission spectrum of the five samples can be seen in Fig. 8. The last figure compares the transmission of sample A1 through the feed line with the transmission through one of the qubit port. Tab. 3 shows the first

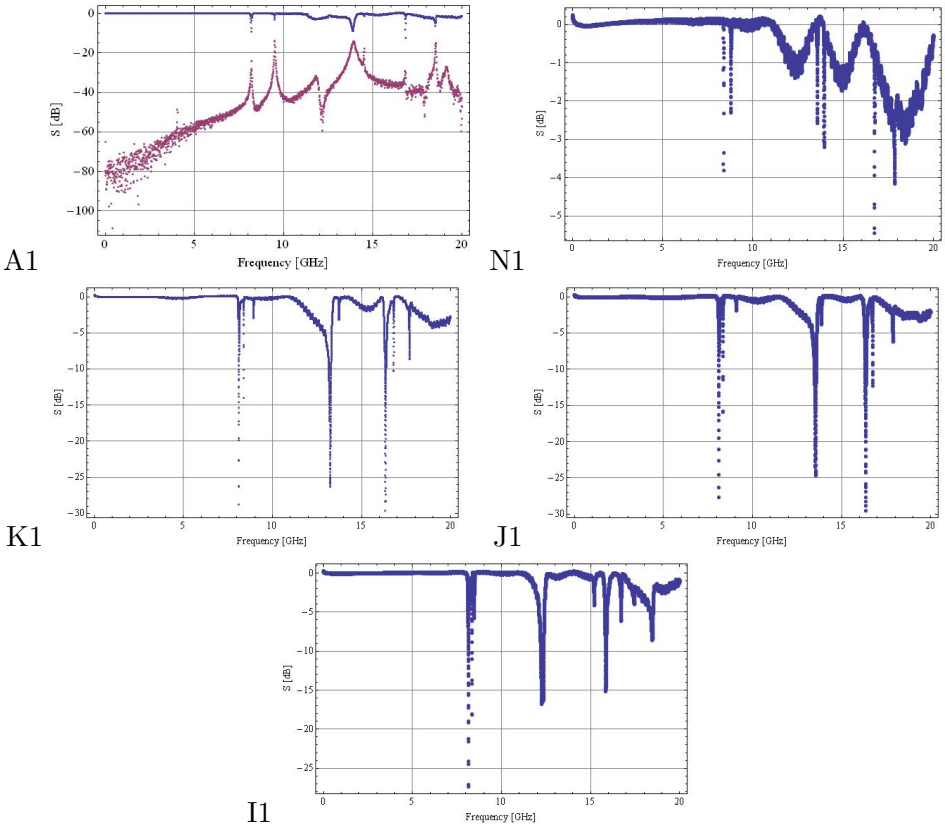

Figure 8: Full transmission spectrum for the samples A1, N1, K1 and J1 with bonds on the ring. The pink line in A1 is the transmission to one of the qubit ports

	ν_0	$\delta\nu$	Q-factor
A1	8.1884	0.0259326	157.878
K1	8.1168	0.0300947	134.855
J1	8.11416	0.0275588	147.216
N1	8.37294	0.00125533	3334.95
I1	8.14464	0.0336428	121.046

Table 3: The first peak in the transmission spectrum with bonds around the ring

resonance point in the transmission spectrum.
The spectrum of K1 and J1 look similar again. What indicates, that the distance of the feed line and the resonator has also with bonds on the ring not a big influence on the spectrum. The number of resonance points is decreasing compared with the measurements without the bonds and the first resonance point is now at 8.11 GHz, what is near to the expected value of 8.2 GHz. Also the second mode at 16.35 GHz can be seen. What is not expected, is that the first and the second mode are subdivided in three peaks, which lie near together and there is a resonance point between the first and the second mode around 13 GHz.
The resonances of sample N1 are even weaker than without bonds and much weaker than in the samples K1 and J1. But like in the other two samples the number of resonances is also decreased and there are double resonances around 8 GHz, 16 GHz and 13 GHz.
The sample A1 was this time measured at all four ports. The resonances are now much weaker than before. The resonance points are still at the expected position, except for the resonance around 13 GHz. Fig. 8 shows also a second spectrum for A1, which is the transmission to the qubit port. The transmission is low, except for the resonance points. What proves, that the resonances are caused by the ring.
The spectrum of I1 is similar to K1 and J1, except for the Q-factors. What is expected, because as already said, the distance between the resonator and the feed line seems to have no influence on the spectrum. The little different can be explained by the different bond configuration.

4.3 Bonds over the Feed line

So far all the bonds were over the resonator. In the next experiment the bonds are added over the feed line. The bonds on the ring are of course still there. The transmission of sample A1 is again measured in all available ports.

The spectrum of all the samples are showed in Fig. 9 and it looks similar to spectrum in the last measurement. The resonance points are still strong for the samples K1 and J1, but weak for A1 and N1. The position of the expected resonances stayed at the same place. The unexpected resonances around 13 GHz seem to vanish. New resonances around 10 GHz and 15 GHz appeared in the samples K1, N1 and J1. If they are really new resonances or if the resonances around 13 GHz are just displaced, is difficult to say.
The transmission through the feed line of sample A1 shows just the two ex-

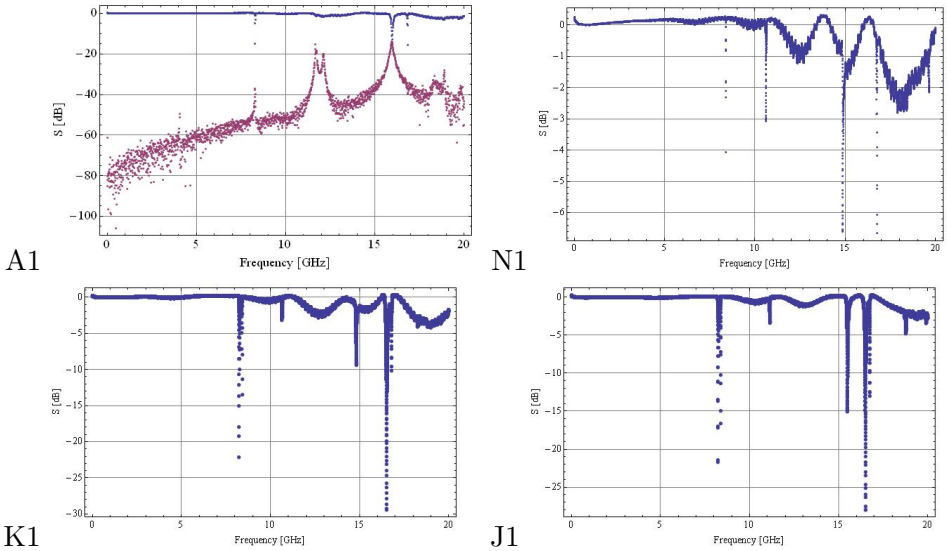

Figure 9: Full transmission spectrum for the samples A1, N1, K1 and J1 with bonds on the ring and on the feed line. The pink line in A1 is the transmission to one of the qubit ports

pected resonances around 8 GHz and 16 GHz, but the transmission trough the qubit port shows also a strong resonance around 12 GHz, what implies, that there is still a resonance, which does not appear in the feed line transmission.
In all four samples the number of resonance is decreasing by adding bonds on the feed line. Tab. 4 shows the position of the first and the second mode. The frequency of the first resonance increased a bit. The frequency of the second mode is nearly double of the frequency of the first mode.

4.4 Bonds over the Ring-Line-Coupling

The most important positions on the samples are the coupling regions of the feed line and the resonator. Now a single bond is added there to the four samples (see appendix Fig. 15). A new sample, called G1, is introduced (see Tab. 1). It is similar to A1, but it has a wall instead of a gap. It has the same bond configuration like the other four samples. The second measurement of I1 is also compared to this measuring sequence, because it has similar bond configuration (see appendix Fig. 15).

	ν_0	$\delta\nu$	Q-factor
A1	8.28678	0.0118685	349.108
	16.8215	0.0165003	509.733
K1	8.402	0.004243	1092.8
	16.5328	0.0582919	141.8
J1	8.24164	0.0139887	294.583
	16.5126	0.0705596	117.012
N1	8.37218	0.00121507	3445.14
	16.7407	0.00348421	2402.37

Table 4: The first and the last mode in the transmission spectrum with bonds around the ring

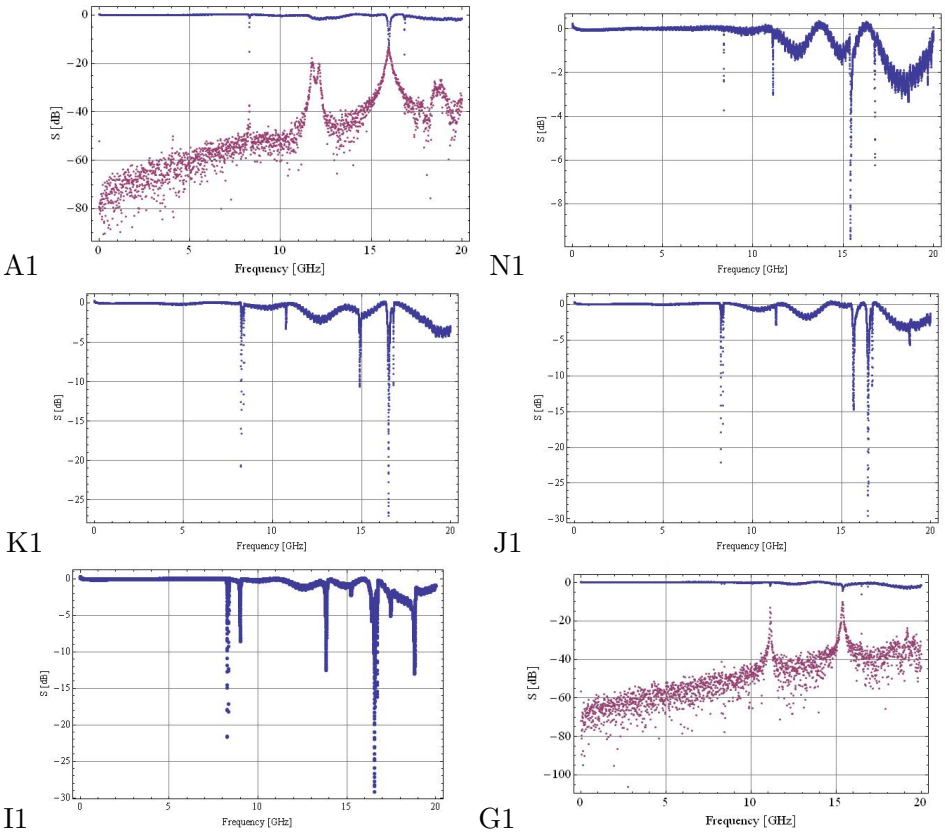

Figure 10: Full transmission spectrum for the samples A1, N1, K1 and J1 with bonds on the ring and on the feed line. The pink line in A1 is the transmission to one of the qubit ports

	ν_0	$\delta\nu$	Q-factor
A1	8.28863	0.0117443	352.88
K1	8.24729	0.0131852	312.747
J1	8.23072	0.0136277	301.984
N1	8.3721	0.00120521	3473.3
G1	8.25851	0.00113365	3642.44
I1	8.27108	0.015115	273.604

Table 5: The first in the transmission spectrum with bonds over the Ring-Line-Coupling

The transmission spectrum is showed in Fig. 10 and it can be seen, that it has not much change for the four samples N1, K1, J1 and A1. Although the new bond was placed on a such important position.
The sample I1 has more peaks, than the others and also one around 13 GHz. This could be explained by fact, that I1 has fewer bonds on the ring and on the feed line than the other samples.
The sample G1 has nearly no resonance in the transmission though the feed line. It has a wall between the feed line and the resonator and two qubit gaps. This two properties made the resonance weaker before and therefore this was expected. The transmission through the qubit port has two strong resonance around 11 GHz and 16 GHz.
Tab. 5 shows the position of the first mode for each sample.

4.5 Final Bond Configuration

So far the transmission spectrum were sometimes very similar and it was decided, that it is useless to measure the same bond configuration for each sample. Therefore in the last measurement sequence there are different bond configurations between the samples.
At I1 bonds are added on the ring and the resonator. At K1 and N1 the bonds are added only on the resonator and at J1 only on the feed line. On sample A1 there are bonds between the qubit gaps and the qubit ports. Pictures of the samples can be seen in the appendix Fig. 16.

The spectrum showed in Fig. 11 looks very similar for the the samples A1, K1, J1 and N1. In the case of K1, J1 and N1 this can be interpret as a saturation. The spectrum does not change anymore, when there are enough bonds on the sample. This point was not reached for the sample I1 in the last experiment and so the spectrum changed for this sample. There are,

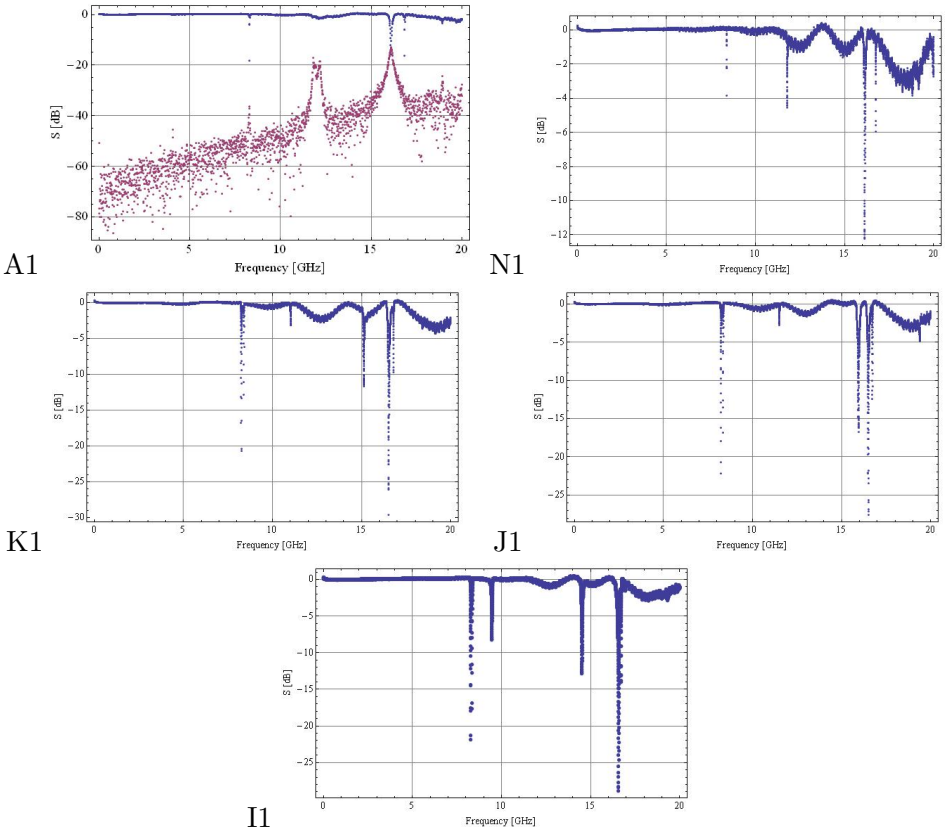

Figure 11: Full transmission spectrum for the samples A1, N1, K1 and J1 with different bond configuration (see appendix). The pink line in A1 is the transmission to one of the qubit ports

	ν_0	$\delta\nu$	Q-factor
A1	8.28955	0.0117333	353.25
K1	8.24865	0.0123981	332.658
J1	8.23211	0.0134152	306.821
N1	8.37206	0.00122496	3417.27
I1	8.27345	0.0144323	286.63

Table 6: The first in the transmission spectrum with the final bond configuration

like expected, fewer peaks than before.
Also bonds between the qubit gap and qubit port seem not to affect the spectrum.
Tab. 6 shows the positions of the first resonances.

5 Simulation

5.1 Simulation Set-up and Results

The transmission spectrum of sample I1 is not just measured, but also simulated. The computer program used for this is called Sonnet and is able to simulate the propagation of microwaves in a coplanar waveguide. The input data consists of the geometry and the material properties of the sample.

The properties of the sample I1 are showed in Tab. 1. There are four simulations of sample I1. First there is a simulation without bonds on the sample. This simulation can not be compared to a measurement of sample I1 directly, because I1 was not measured without bonds. But in the last section, it was shown, that the distance between the feed line and the ring has not a big influence on the spectrum and therefore this simulation is compared to J1 (Fig. 6 J1).
The second measurement is made with the same bond configuration like the first measurement of I1. Therefore the spectrum is compared to Fig. 8 I1. The bonds were considered to be superconducting, what obviously is not true.
Therefore the third simulation has the same bond configuration, but now the bonds are defined to have a resistivity of $0.82 \cdot 10^{-3}$ $\mu\Omega$m, which is the resistivity of aluminum in the measurements (at 4 K) [9].
In the last simulation the bond configuration is like the one in the second measurement of I1 and therefore the spectrum is compared to Fig. 10 I1. The resistivity of the bonds is still $0.82 \cdot 10^{-3}$ $\mu\Omega$m.
Pictures of both bond configurations are in the appendix Fig. 13 and Fig. 15.

Sonnet calculates the transmission just for few frequencies. Therefore the figures showed in the next section just show few points, which are connected by lines. The distance between two points is to wide to see double peaks or determine the Q-factor. But it can be guessed, where the resonance point are. The results are therefore inexact.

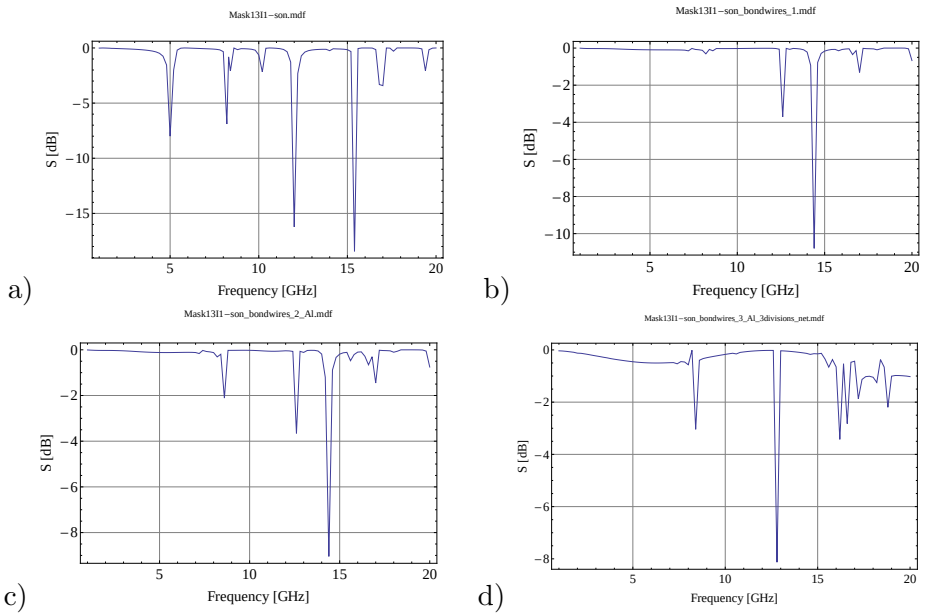

Figure 12: Simulated spectrum of sample I1 with a) no bonds, b) with superconducting bonds, c) aluminum bonds and d) with a different aluminum bond configuration.

5.2 Results and Comparison to the Measurements

The results of the simulations are showed in Fig. 12. The first picture a) shows the resonances without bonds on the sample. There are many resonance points between 5 and 20 GHz, what was expected for a sample without bonds. It looks similar to Fig. 6 J1, even the resonance points are not exact on the same position.
The second simulation with the superconducting bonds is showed in b). There are only two clear peaks, both in the region between 12 and 15 GHz. This might be the 13 GHz peak from the measurement and the shifted second mode. The first mode does not appear in this simulation, what may be caused by the large distance between two simulated frequencies.
The simulation is repeated with aluminum instead of superconducting bonds. The spectrum is showed in c). It looks similar to the last one, except the first mode can be seen this time. The peaks are nearly on the same position as in the measurement. This implies, that the 13 GHz peak is not a measurement error.
The last simulation with the second bond configuration is showed in d). The first and second mode can be seen in the simulation. The peak between is still there. It is shifted a bit to lower frequency compared to the measurement.

6 Summary and Outlook

The goal of this experiment was to understand the microwave properties of a ring resonator without qubits for different geometry set-ups and different numbers of bond wires. The first result seen in the experiment was, that the distance between the resonator and the feed line in the sample with a gap did not have a influence on the transmission spectrum, but changing the Q-factors. If this would also be true in the case at samples with a wall between the resonator and feed line, was not measured in this experiment.
A sample with a wall has, compared to a sample with a gap, weaker resonances. This is particularly important, because also a qubit gap is decreasing the magnitude of resonances and in combination the signal nearly vanish. The advantage of qubit gaps is, that the number of peaks is reduced and so the goal of only two peaks (first and second mode) is getting closer, except for traces of the peak at 13 GHz.
In general an increase in the number of bonds decreases the number of unexpected peaks. Particularly there has to be enough bonds on the ring and on the feed line to remove most of the unexpected peaks. Bonds on the coupling region of the resonator and the feed line or between the port and the qubit gap are not necessary. Also a sample with too many bonds does not change the transmission spectrum compared to a sample with less bonds. This can be seen a saturation.

The appearance of double and three-way peaks could not be explained and it could also not to be avoid. A possible explanation can be find at [13]. The peak between the first two mode could also not be explained, but this effect could be partly avoid by bonds. A goal of a next experiment could be to explain this two phenomena.
A possible next step in this experiment could also be to add qubits in the qubit gaps and to analyze the coupling to the electromagnetic field mode.

7 Acknowledgments

I thank Prof. Andreas Wallraff for providing the laboratory work in his Quantum Device Lab. I thank also my supervisor Lars Steffen for helping me in this three weeks and for his patience to answer my question. Furthermore I thank the whole Quantum Device Group for their kindness and their support in difficult situations.

8 Bibliography

References

[1] Weblink: http://en.wikipedia.org/wiki/Charge_qubit, 8.4.2011

[2] Blais et al., Physical Review A 69, 062320, 2004

[3] Wallraff et al., Nature (London) 431, 162 , 2004

[4] Majer et al., Nature (London) 449 443, 2007

[5] Weblink: http://en.wikipedia.org/wiki/Waveguide_(electromagnetism), 21.3.2011

[6] Weblink: http://en.wikipedia.org/wiki/Wave_impedance, 21.3.2011

[7] M. Göppl, A Fragner, M. Baur, R. Bianchetti, S. Filipp, J.M. Fink, P.J. Leek, G. Puebla, L Steffen, and A. Wallraff, Coplanar Waveguide Resonators for Circuit Quantum Electrodynamics, July 29, 2008

[8] Weblink: http://en.wikipedia.org/wiki/Niobium, 25.3.2011

[9] A.F. Clarka, G.E. Childsa and G.H. Wallacea, Electrical resistivity of some engineering alloys at low temperatures, Sciencedirect, 1970

[10] Weblink: http://de.wikipedia.org/wiki/Fotolithografie_(Halbleitertechnik), 28.3.2011

[11] Weblink: http://www.microwaves101.com/encyclopedia/coaxloss.cfm, 8.4.2011

[12] A. Wallraff, H. Majer, L. Frunzio, R. Schoelkopf, Superconducting Solid State Cavity Quantum Electrodynamics

[13] S.-L. Lu and A.M. Ferendeci, Coupling modes of a ring resonator side coupled to a microstrip line, Electronics Letter, 1994

9 Appendix

The pictures of the samples with different bond configuration are showed from Fig. 13 to Fig. 16. The samples in bracket are not showed, but has the same bond configuration like the sample showed on the picture.

a) 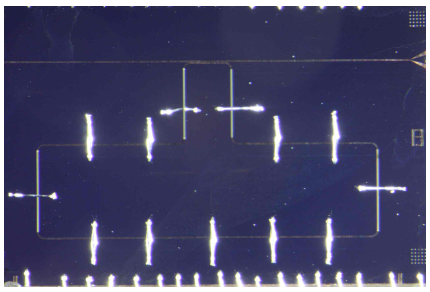 b) 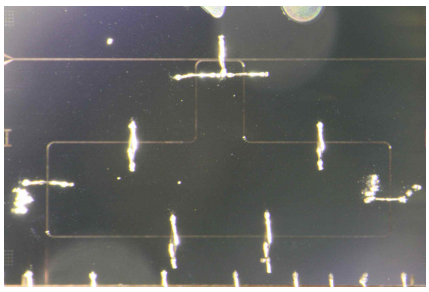

Figure 13: a) Bond configuration of the sample N1(J1,K1,A1) and b) bond configuration of sample I1 in the measurements from section 4.2.

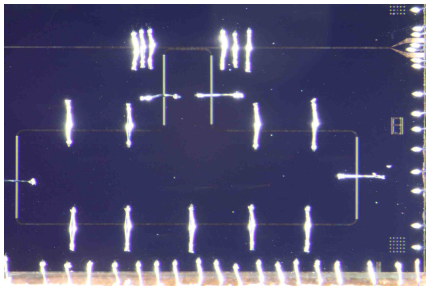

Figure 14: Bond configuration of the sample N1(J1,K1,A1) in the measurements from section 4.3.

a) 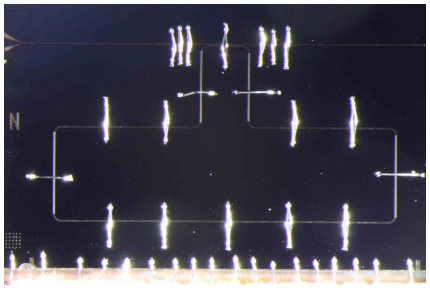 b) 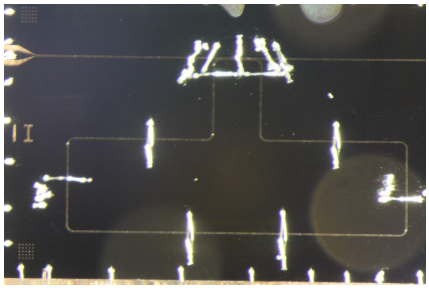

Figure 15: a) Bond configuration of the sample N1(J1,K1,A1) and b) bond configuration of sample I1 in the measurements from section 4.4.

a) 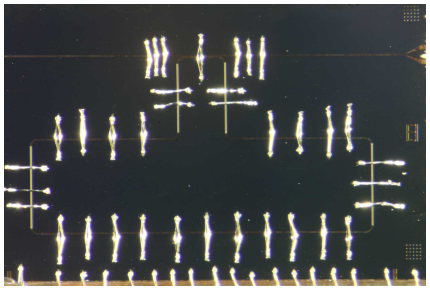 b) 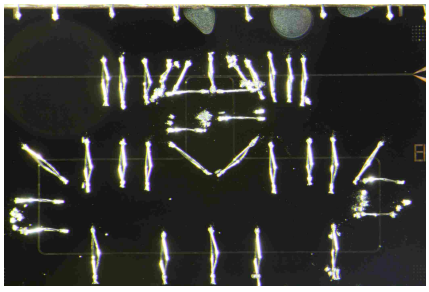

c) 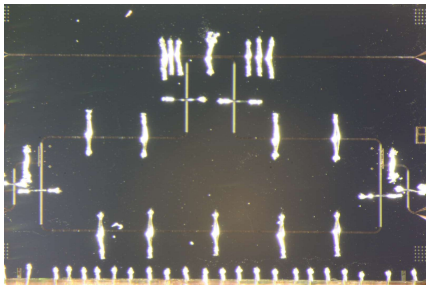 d) 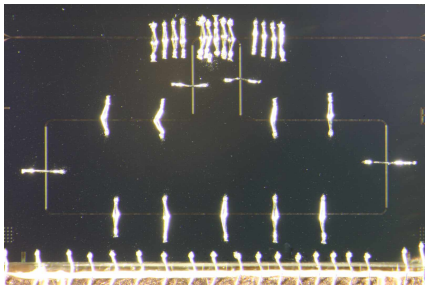

Figure 16: a) Bond configuration of the sample N1(K1), b) bond configuration of sample I1, c) bond configuration of sample A1 and d) bond configuration of sample J1 in the measurements from section 4.5.